

Electronic Supplementary Information:

What can be inferred from moiré patterns?

A case study of trimesic acid monolayers on graphite

Saskia Spitzer,^{a,b} Oliver Helmle,^a Oliver Ochs,^{a,b} Natalia Martsinovich,^c Josh Horsley,^c
Wolfgang M. Heckl,^{a,b} and Markus Lackinger^{a,b*}

^a Department of Physics, Technische Universität München, James-Franck-Str. 1, 85748 Garching, Germany.
Nanosystems-Initiative-Munich and Center for NanoScience, Schellingstrasse 4, 80799 München, Germany.

^b Deutsches Museum, Museumsinsel 1, 80538 München, Germany.

^c University of Sheffield, Sheffield S3 7HF, UK

Additional STM data

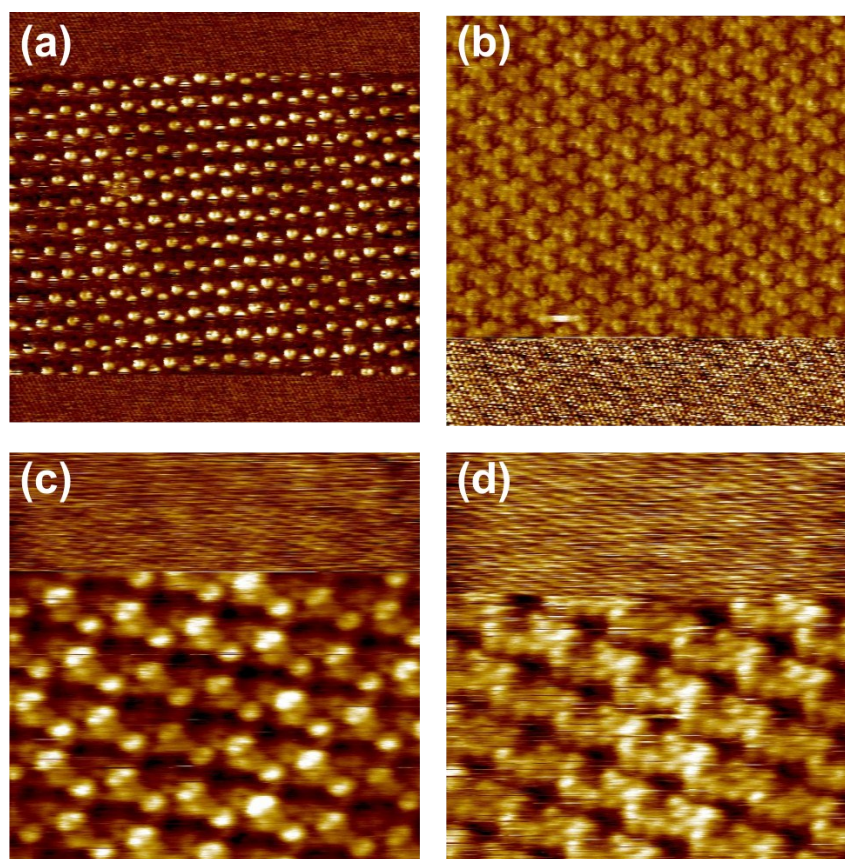


Fig. S1 STM split-images of the TMA chickenwire structure. After imaging the molecular network, the tunneling voltage was lowered in order to obtain atomic resolution of the underlying graphite. From these images the ratio of TMA to graphite lattice parameter $a_{TMA}/a_{graphite}$ as well as the relative rotation angle α can be deduced: (a) solvent: heptanoic acid, saturated solution, $25 \times 25 \text{ nm}^2$, $a_{TMA}/a_{graphite} = 6.61$; $\alpha = 7.2^\circ$; (b) solvent: heptanoic acid, $\sim 20\%$ saturated solution, $20 \times 20 \text{ nm}^2$, $a_{TMA}/a_{graphite} = 6.69$; $\alpha = 5.1^\circ$; (c) solvent: nonanoic acid, saturated solution, applied to hot surface, $10 \times 10 \text{ nm}^2$,

$a_{TMA}/a_{graphite} = 6.72$, $\alpha = 5.2^\circ$; (d) solvent: nonanoic acid, saturated solution, applied to hot surface, $10 \times 10 \text{ nm}^2$,
 $a_{TMA}/a_{graphite} = 6.79$, $\alpha = 5.4^\circ$;

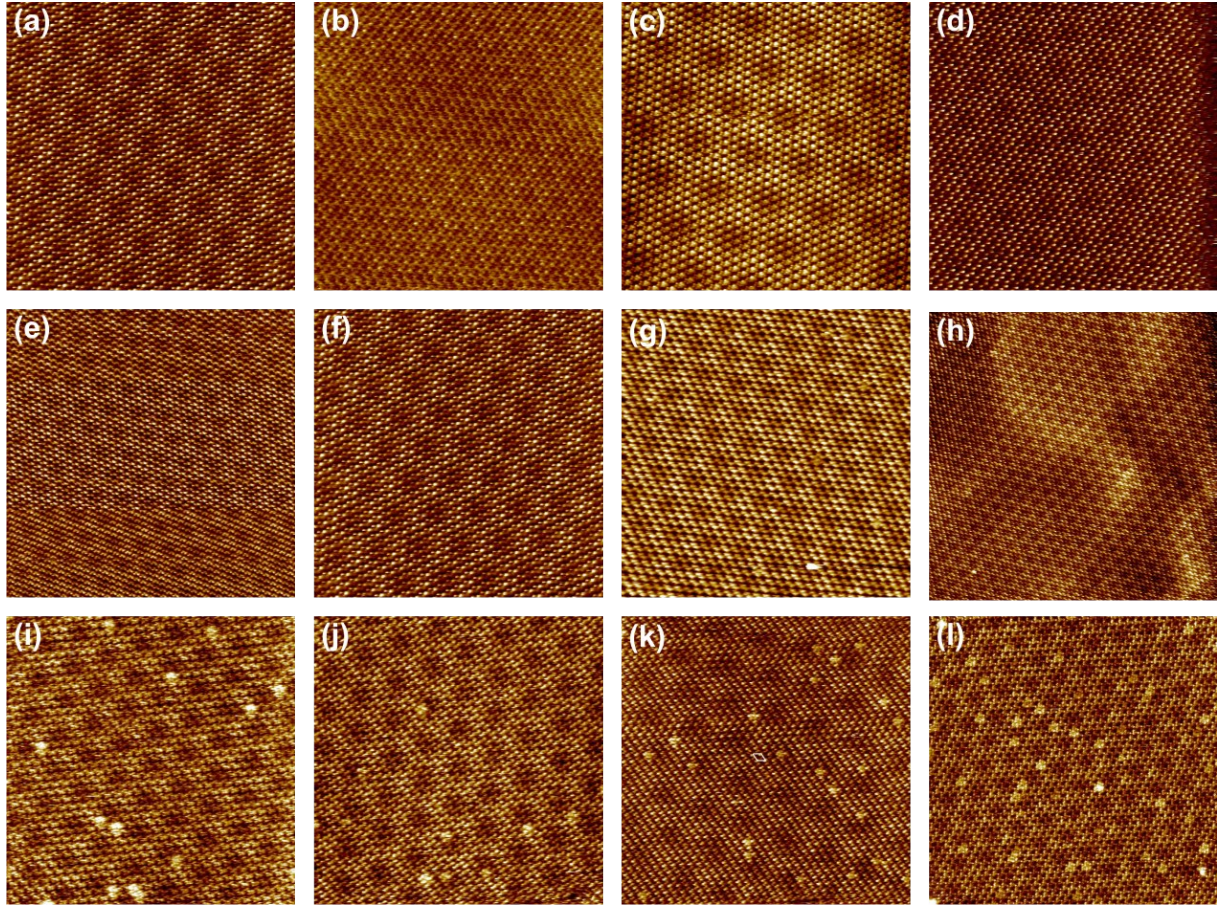


Fig. S2 Large scale STM images of the TMA chickenwire structure with clearly visible moiré patterns. These images were evaluated for the plot shown in the main paper in Fig. 6: (a) solvent: heptanoic acid, saturated solution ($50 \times 50 \text{ nm}^2$, -600 mV , 52 pA), $A_{\text{moiré}} = 6.99 \text{ nm}$, $\varphi = 18.9^\circ$; (b) solvent: heptanoic acid, 20% saturated solution ($50 \times 50 \text{ nm}^2$, -500 mV , 45 pA), $A_{\text{moiré}} = 5.02 \text{ nm}$, $\varphi = 4.2^\circ$; (c) solvent: heptanoic acid, saturated solution ($50 \times 50 \text{ nm}^2$, -550 mV , 52 pA), $A_{\text{moiré}} = 9.30 \text{ nm}$, $\varphi = 39.3^\circ$; (d) solvent: heptanoic acid, saturated solution ($50 \times 50 \text{ nm}^2$, -612 mV , 51 pA), $A_{\text{moiré}} = 7.03 \text{ nm}$, $\varphi = 21.2^\circ$; (e) solvent: heptanoic acid, saturated solution ($70 \times 70 \text{ nm}^2$, -566 mV , 54 pA), $A_{\text{moiré}} = 6.51 \text{ nm}$, $\varphi = 16.4^\circ$; (f) solvent: heptanoic acid, saturated solution ($50 \times 50 \text{ nm}^2$, -588 mV , 52 pA), $A_{\text{moiré}} = 6.94 \text{ nm}$, $\varphi = 19.1^\circ$; (g) solvent: nonanoic acid, saturated solution, applied to hot surface ($50 \times 50 \text{ nm}^2$, -606 mV , 52 pA), $A_{\text{moiré}} = 6.01 \text{ nm}$, $\varphi = 12.7^\circ$; (h) solvent: nonanoic acid, saturated solution, applied to hot surface ($100 \times 100 \text{ nm}^2$, -588 mV , 52 pA), $A_{\text{moiré}} = 5.01 \text{ nm}$, $\varphi = 6.5^\circ$; (i) solvent: nonanoic acid, saturated solution, applied at room temperature ($50 \times 50 \text{ nm}^2$, -588 mV , 53 pA), $A_{\text{moiré}} = 6.13 \text{ nm}$, $\varphi = 15.1^\circ$; (j) solvent: nonanoic acid, saturated solution, applied at room temperature ($50 \times 50 \text{ nm}^2$, -600 mV , 52 pA), $A_{\text{moiré}} = 6.67 \text{ nm}$, $\varphi = 16.7^\circ$; (k) solvent: nonanoic acid, saturated solution, applied at room temperature ($70 \times 70 \text{ nm}^2$, -600 mV , 52 pA), $A_{\text{moiré}} = 9.06 \text{ nm}$, $\varphi = 34.9^\circ$; (l) solvent: nonanoic acid, saturated solution, applied at room temperature, but STM image acquired at 50°C ($60 \times 60 \text{ nm}^2$, $+630 \text{ mV}$, 56 pA), $A_{\text{moiré}} = 5.97 \text{ nm}$, $\varphi = 12.6^\circ$;

Additional Simulations

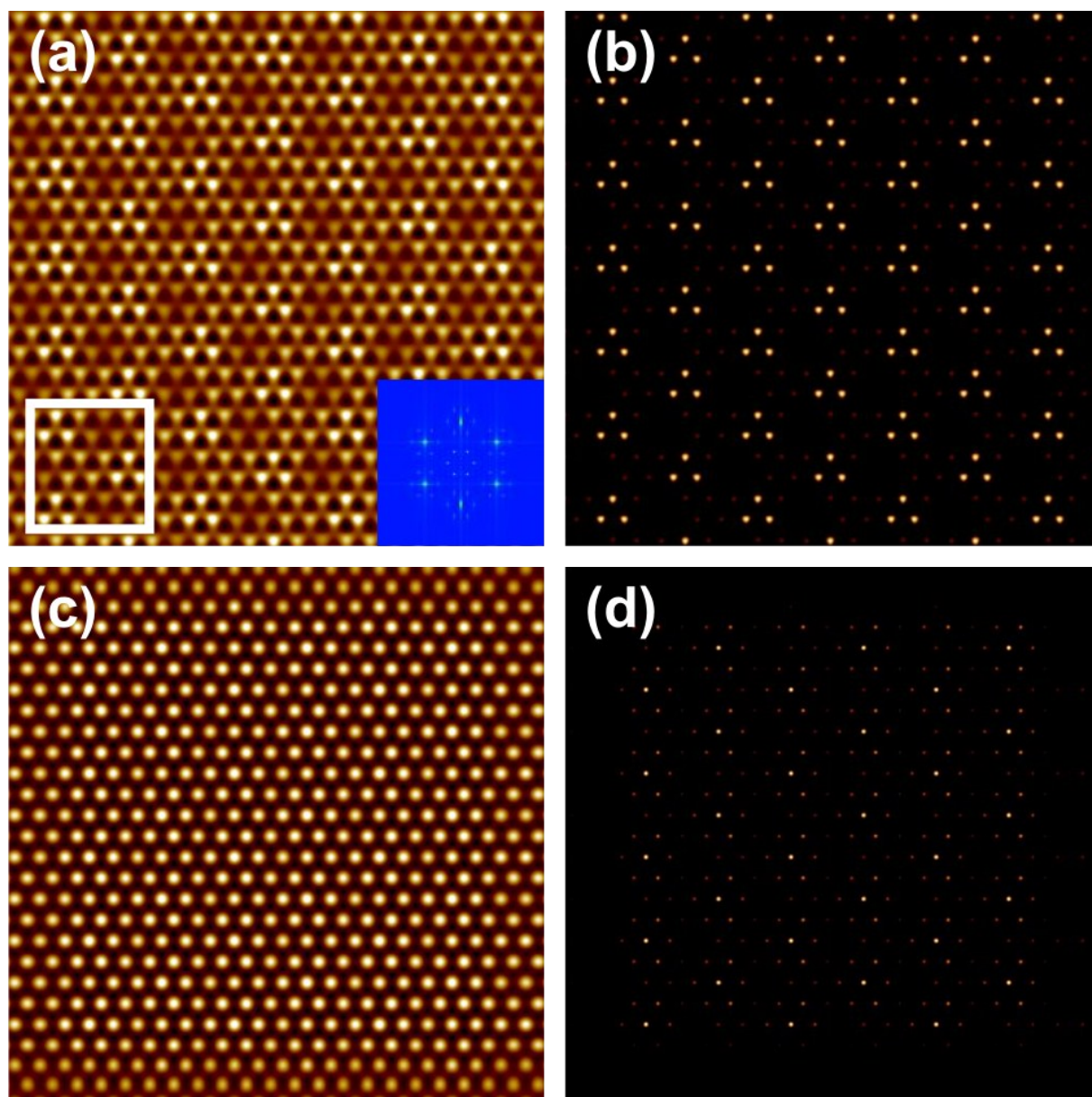


Fig. S3 Image processing of a simulated commensurate moiré pattern (a) original image, the inset depicts the corresponding FFT. (b) Same image with adjusted colour-scale to highlight the topographic maxima. Similar appearing groups of three maxima are repeated with the moiré periodicity, indicating a fully periodic structure. (c) cross-correlation of the main image (a) with the close-up marked by the rectangle. (d) same cross-correlation with adjusted colour-scale to highlight intensity maxima. Positions of the maxima are distributed with the lattice symmetry of the underlying structure with smaller lattice parameter. However, highest intensities are observed for simultaneous coincidence of moiré and base structure. These higher intensities appear with a regular distribution of the moiré lattice without any decay across the cross-correlation.

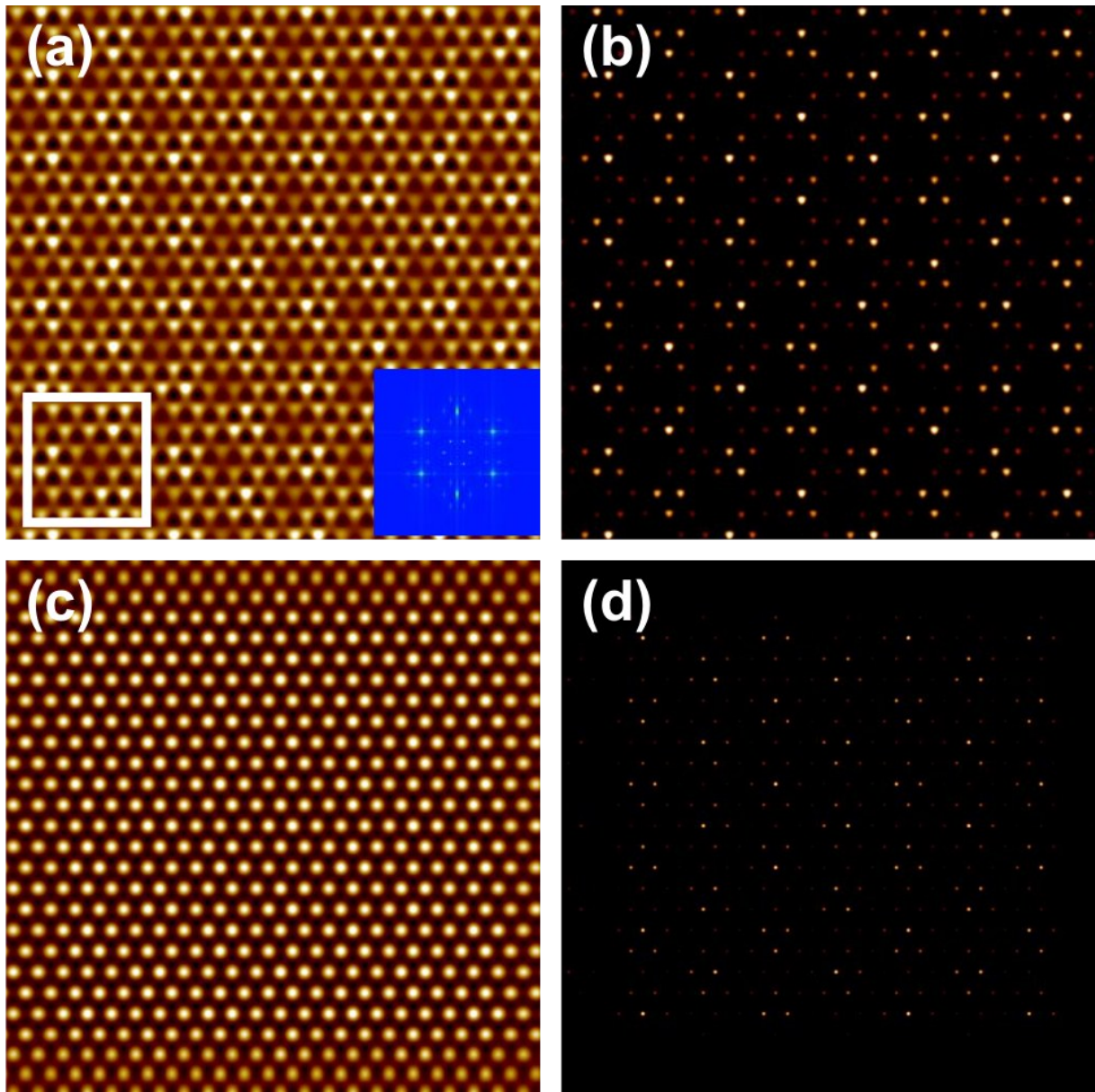


Fig. S4 Image processing of a simulated incommensurate moiré pattern (a) original image, the inset depicts the corresponding FFT. (b) Same image with adjusted colour-scale to highlight the topographic maxima. Groups of maxima are distributed on moiré lattice points. However, these groups are not similar in appearance, indicating a lack of translational symmetry for the incommensurate moiré pattern. (c) cross-correlation of the main image (a) with the close-up marked by the rectangle. (d) same cross-correlation with adjusted colour-scale to highlight the maxima. Positions of the maxima are distributed with the lattice symmetry of the underlying structure with smaller lattice parameter. However, the highest intensity is only observed at the original position of the close-up. In contrast to the commensurate moiré, there is no further point where moiré and base structure coincide simultaneously. Consequently, this original intensity cannot be regained anymore and the intensities decay away from the original position due to increasing dephasing. Direct comparison to the commensurate case in Fig. S3 illustrates the differences for commensurate vs. incommensurate moiré patterns.

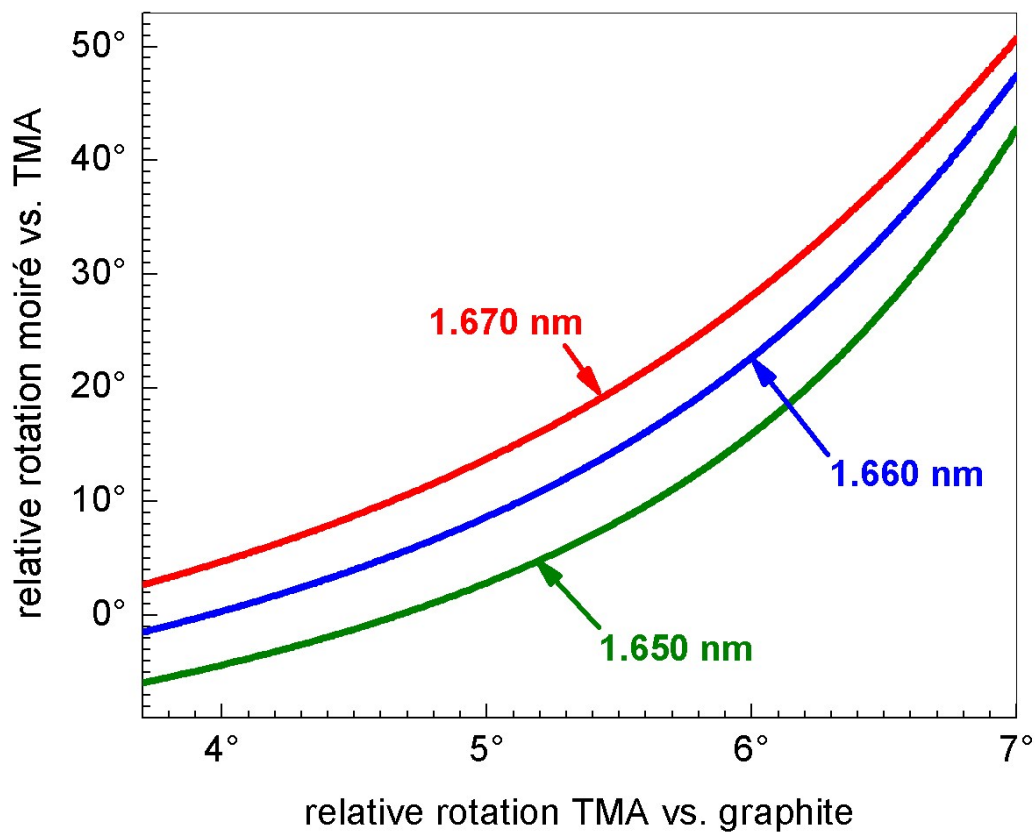


Fig. S5 Theoretical curves for the relative rotation angle φ between moiré and TMA lattices as a function of relative rotation α between TMA and graphite lattices around the experimental value $\alpha=5^\circ$. The plot is based on the reciprocal space construction shown in Fig. 3 of the main article and assumes the closest proximity between (1,0) graphite and (7,1) TMA Fourier components, respectively. The moiré orientation also sensitively depends on the TMA lattice parameter as illustrated by the different curves for specific a_{TMA} as indicated.